Oncogene (2000) 19, 1215–1224
© 2000 Macmillan Publishers Ltd All rights reserved 0290–9232/00 $15.00
www.nature.com/onc

Developmental expression of Pim kinases suggests functions also outside of the hematopoietic system

Anne Eichmann*[,1], Li Yuan[1], Christiane Bréant[1], Kari Alitalo[2] and Päivi J Koskinen[3]

[1]*Institut d'Embryologie Cellulaire et Moléculaire du CNRS et du Collège de France 49bis, Avenue de la Belle Gabrielle, 94736 Nogent-sur-Marne Cedex, France;* [2]*Haartman Institute, University of Helsinki, 00014 Helsinki, Finland;* [3]*Turku Centre for Biotechnology, University of Turku/Åbo Akademi University, Tykistökatu 6 B, 20520 Turku, Finland*

We have cloned a novel quail cDNA with strong homology to the *pim* family of proto-oncogenes. The deduced amino acid (aa) sequence of the cDNA, named *qpim*, is more closely related to *Xenopus* Pim and to the recently identified rat Pim-3 than to human or rodent Pim-1 or Pim-2. The protein encoded by the *qpim* cDNA can autophosphorylate itself and share substrates with murine Pim-1, suggesting functional redundancy to other Pim family serine/threonine kinases. We have compared the expression of *qpim* in avian embryos to mouse *pim-1*, *-2* and *-3* by *in situ* hybridization. *qpim* shows a highly dynamic expression pattern, particularly at early developmental stages. Surprisingly, its expression pattern is not identical to any of the murine *pim* genes, which show complementary and/or partially overlapping expression sites both in- and outside of the hematopoietic system. Altogether, our results suggest novel functions for Pim family kinases during embryonic development, in particular in epithelia and in the central nervous system. *Oncogene* (2000) **19,** 1215–1224.

Keywords: pim kinases; quail; expression; embryonic development

Introduction

The *pim* family proto-oncogenes encode serine/threonine-specific kinases (Saris *et al*., 1991; Hoover *et al*., 1991; van der Lugt *et al*., 1995). The first member of the family, *pim-1*, was originally identified as a common proviral insertion site in Moloney murine leukemia virus-induced T-cell lymphomas in mice (Cuypers *et al*., 1984). Proviral integration was found to occur mostly in the 3′ untranslated region of *pim-1* (Selten *et al*., 1985), resulting in overexpression of the *pim-1* mRNA and protein. The oncogenic potential of the *pim-1* gene in the lymphoid compartment was further proven with Eμ-*pim-1* transgenic mice which developed T-cell lymphomas, albeit with low incidence and long latency (van Lohuizen *et al*., 1989). This suggested that overexpression of the *pim-1* gene by itself was insufficient for cell transformation. Accordingly, when Eμ-*pim-1* mice were exposed to viral or chemical carcinogenic agents, the development of lymphomas was accelerated (van Lohuizen *et al*., 1989; Breuer *et al*., 1989). In most cases, this correlated with activation of one of the *myc* family oncogenes. The capacity of *pim-1* and *myc* to synergize in lymphomagenesis was most convincingly shown with crosses of Eμ-*pim-1* and Eμ-*myc* transgenic mice which resulted in development of lymphoid malignancies already in utero (Möröy *et al*., 1991; Verbeek *et al*., 1991). *pim-1* has been shown to cooperate in lymphomagenesis also with *bcl-2* (Acton *et al*., 1992), suggesting that overexpression of *pim-1* can enhance or complement the effects of two types of oncogenes that either promote cell proliferation (*myc*) or cell survival (*bcl-2*). While the mechanisms of oncogene cooperation still remain unclear, experimental evidence indicates that Pim-1 can enhance the activity of some transcription factors such as c-Myb (Leverson *et al*., 1998) and NFATc1 (EM Rainio, J Sandholm and PJ Koskinen, in preparation). Pim-1 can also inhibit certain types of apoptosis in hematopoietic cells (Möröy *et al*., 1993; Lilly and Kraft, 1997; Lilly *et al*., 1999).

pim-1 has been reported to be expressed mainly in hematopoietic tissues and in testis in both mouse and man (Meeker *et al*., 1987; Sorrentino *et al*., 1988; Amson *et al*., 1989; van Lohuizen *et al*., 1989; Wingett *et al*., 1992). In hematopoietic cell lines, *pim-1* expression can be induced by multiple cytokines (Dautry *et al*., 1988; Lilly *et al*., 1992; Matikainen *et al*., 1999), suggesting that the Pim-1 kinase may be an important intermediate in signal transduction initiated by cytokine receptors. *pim-1* expression is also induced during T-cell activation (Wingett *et al*., 1996). During human fetal hematopoiesis, Pim-1 protein is highly expressed in liver and spleen, as shown by immunohistochemical staining, while in the adult, the protein has been detected only in circulating granulocytes (Amson *et al*., 1989). By contrast, high levels of *pim-1* mRNA and protein are expressed in cell lines and tissues from human patients with lymphoid or myeloid malignancies (Meeker *et al*., 1987; Amson *et al*., 1989), suggesting that inappropriate overexpression of *pim-1* may contribute to cell transformation also in humans.

Null mutants of the *pim-1* gene, generated by targeted gene inactivation (te Riele *et al*., 1990), were phenotypically surprisingly normal with only few changes in their hematopoietic compartment (Laird *et al*., 1993; Domen *et al*., 1993a,b). The minor consequences of gene inactivation compared to the profound effects caused by *pim-1* overexpression suggested the presence of functionally redundant genes. Indeed, a highly homologous family member, *pim-2*, was subsequently isolated by degenerate-primer PCR using DNA isolated from *pim-1*-deficient mice (van der Lugt *et al*., 1995). More recently, another serine/threonine kinase with high homology to Pim-1 was described (Feldman *et al*., 1998a). This kinase named Kid-1 (for *k*inase *i*nduced by *d*epolarization) was

*Correspondence: A Eichmann
Received 15 January 1999; revised 28 October 1999; accepted 14 November 1999

identified by a differential screen designed to identify depolarization-induced mRNAs from rat PC12 cells. The *kid-1* gene is identical to rat *pim-3* isolated in a low-stringency homology search for additional *pim* family members (Konietzko *et al*., 1999). Comparisons of the tissue distributions of *pim* family mRNAs in adult mice or rats revealed partially overlapping expression patterns not only in hematopoietic tissues, but also in brain (Allen *et al*., 1997; Feldman *et al*., 1998b; Konietzko *et al*., 1999).

We here report the cloning of a *pim*-like cDNA from a quail library. The protein product encoded by this cDNA shows strongest sequence similarity to *Xenopus* Pim and rat Pim-3, and a lesser degree of homology to mammalian Pim-1 and Pim-2. We have also analysed and compared the expression patterns of quail *qpim* and mouse *pim-1*, *-2* and *-3* by *in situ* hybridization in developing embryos. The different expression patterns of quail and mouse genes are consistent with two hypotheses: either the functions of Pim kinases are not conserved between murine and avian species, or Qpim represents a fourth Pim kinase family member.

Results

Cloning of the qpim *gene*

Low-stringency screening of an embryonic day 4 (E4) quail cDNA library (see Materials and methods) yielded a 2.3 kb clone with high homology to the *pim* gene family of protein kinases. The cDNA named *qpim* was subsequently sequenced on both strands and found to contain a single open reading frame predicted to code for a protein of 323 amino acids (aa) (Figure 1a). Comparison of the deduced aa sequence of Qpim to known Pim family proteins showed that quail and *Xenopus* Pim sequences are 87% identical and completely colinear (Figure 1a,b). The second closest homolog to Qpim is the recently identified rat Kid-1/Pim-3 kinase (Feldman *et al*., 1998a; Konietzko *et al*., 1999) with 81% aa identity. The other Pim family kinases are evolutionarily more diverged, with Qpim having 67–68% aa identity to human, rat and mouse Pim-1 and only 53–54% aa identity to the corresponding Pim-2 proteins. Cross-comparison of the different Pim family members (Figure 1b) indicated that the degree of aa identity between *Xenopus* Pim-1, rat Pim-3 and quail Qpim is around 80%, whereas these three proteins are 65–69% identical to human, mouse and rat Pim-1 and 50–57% identical to human and mouse Pim-2.

Northern blot analysis with the entire quail cDNA revealed a single transcript of about 3 kb that was present in quail E4 embryonic RNA as well as in adult brain and kidney (not shown). The size of the transcript suggested that part of the untranslated quail *qpim* sequences were missing from the isolated 2.3 kb cDNA fragment.

Functional characterization of the Qpim protein

To determine whether the *qpim* cDNA produced an active kinase, we compared the *in vitro* kinase activities of bacterially expressed GST fusion proteins encoding either Qpim or mouse Pim-1. As shown in Figure 2, both of them were able to autophosphorylate. The quail GST-Qpim protein migrated more slowly than murine Pim-1, due to additional amino acids in the linker region between GST and Qpim. Both quail and murine kinases were also able to phosphorylate exogenous substrates. These included histone H1 (not shown) as well as a GST fusion protein of NFATcl (nuclear factor of activated T cells; Figure 2). Neither kinase phosphorylated non-recombinant GST protein, confirming the specificities of the observed phosphorylation events. Also, a K67M kinase-deficient mutant of murine Pim-1 remained inactive in all these assays (not shown). Altogether, our results confirmed that we had isolated a functional *qpim* gene from the quail library.

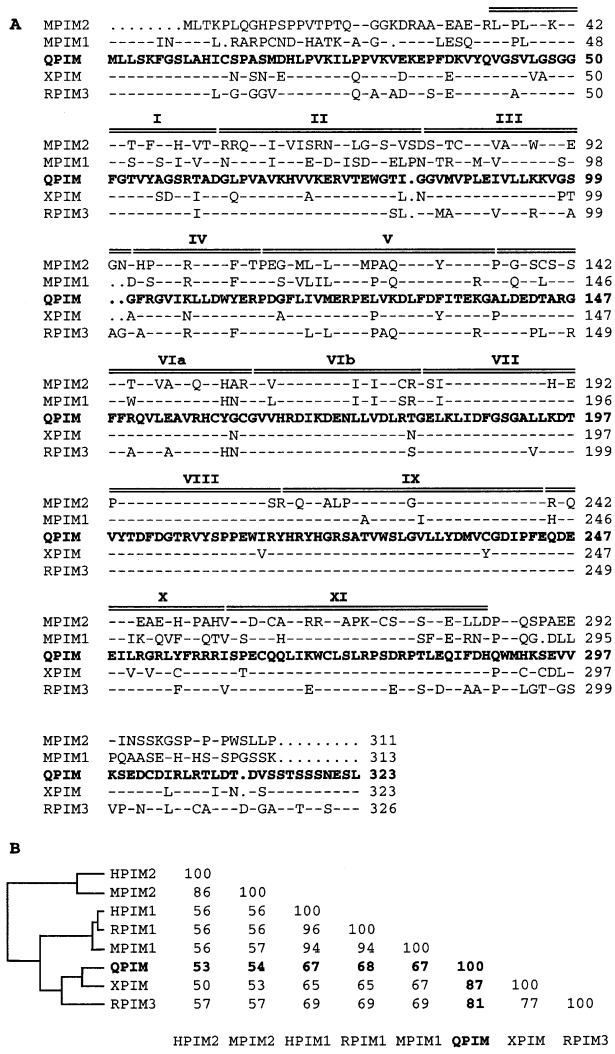

Figure 1 The isolated quail cDNA encodes a Pim family kinase. (**a**) Amino acid comparison of the quail Qpim protein (QPIM) to other Pim family proteins, including murine Pim-2 (MPIM2) and Pim-1 (MPIM1), *Xenopus* Pim (XPIM) and rat Pim-3 (RPIM3). The aa residues identical to Qpim are indicated with dashes and the missing residues with dots. Catalytic subunits typical for protein kinases are indicated by Roman numerals above the aligned sequences. The nucleotide sequence of the *qpim* cDNA has been deposited to the EMBL database (accession no. AJ130845). (**b**) Phylogenetic tree of known vertebrate Pim family proteins and their degrees of identity to each other in percentages. In addition to sequences compared in **a**, rat Pim-1 (RPIM1), human Pim-1 (HPIM1) and Pim-2 (HPIM2) proteins have also been included

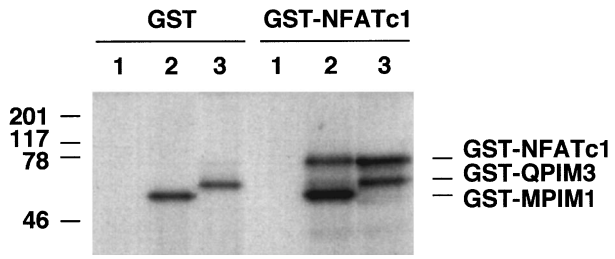

Figure 2 The quail Qpim is able to phosphorylate both itself and NFATc1. The *in vitro* kinase activities of murine and quail GST-Pim proteins were analysed with GST-NFATc1 (aa 1–418) as an exogenous substrate. 1, GST; 2, GST-MPIM1; 3, GST-QPIM. The molecular weight markers are indicated on the left and the positions of the GST fusion proteins on the right

Onset of qpim *expression during embryonic development*

Expression of *qpim* was analysed by whole-mount *in situ* hybridization as well as on sections from E1 to E10 embryos. Digoxygenin-labeled sense and antisense riboprobes were synthesized from the entire cDNA. Sense probes did not show any specific signal (not shown). Quail and chick embryos were examined and no differences between the two species were observed.

qpim was expressed in the embryo from around the 8-somite stage, at which stage the heart starts beating. Prior to this time, no signal was detected (not shown). The yolk sac blood islands were negative for *qpim* expression (Figure 3a). From the 8- to about the 25-somite stage, transcripts were detected in the myocardium, lateral mesoderm and the medial part of the somites (Figure 3a,c–e). These expression sites were transient: the myocardium and lateral mesoderm expressed *qpim* only during a period of about 24 h. In the somites, myotomal cells derived from the medial somitic part were strongly *qpim* positive until E5 (Figure 3b,f). The only early *qpim* expression site which persisted throughout the developmental period examined was the Wolffian duct (Figure 3a,d), which was *qpim* positive from the moment of its formation. The Wolffian duct gives rise to kidney tubules which remained *qpim* positive until at least E10 (see Figure 5a).

During the first 2 days of avian embryonic development, *qpim* expression was thus observed in mesodermal derivatives only. From E3 onward, expression of this gene extended to ectoderm- and endoderm-derived structures.

qpim *expression in ectoderm-derived structures*

At E3, *qpim* started being expressed in the developing central nervous system (CNS, Figure 4a). Expression was observed in the ventral mesencephalon and in the diencephalon in the region of the hypothalamic infundibulum. The developing retina and lens were *qpim* positive as well. In the spinal cord, *pim-1* expression was first observed in the forming motoneuron columns and in the floor plate (Figure 4a). At E5, *qpim* expression in the developing CNS had extended significantly and was observed in migrating and differentiating neurons (Figures 4b,c and 5a,b). The neurohypophysis (Figure 4c) and adenohypophysis were *qpim* positive. The neural retina also showed strong *qpim* expression until at least E7. From E5 onward, the olfactory epithelium expressed *qpim* in the region of developing olfactory neurons (Figure 4d). In contrast, the region of developing nasal epithelium was

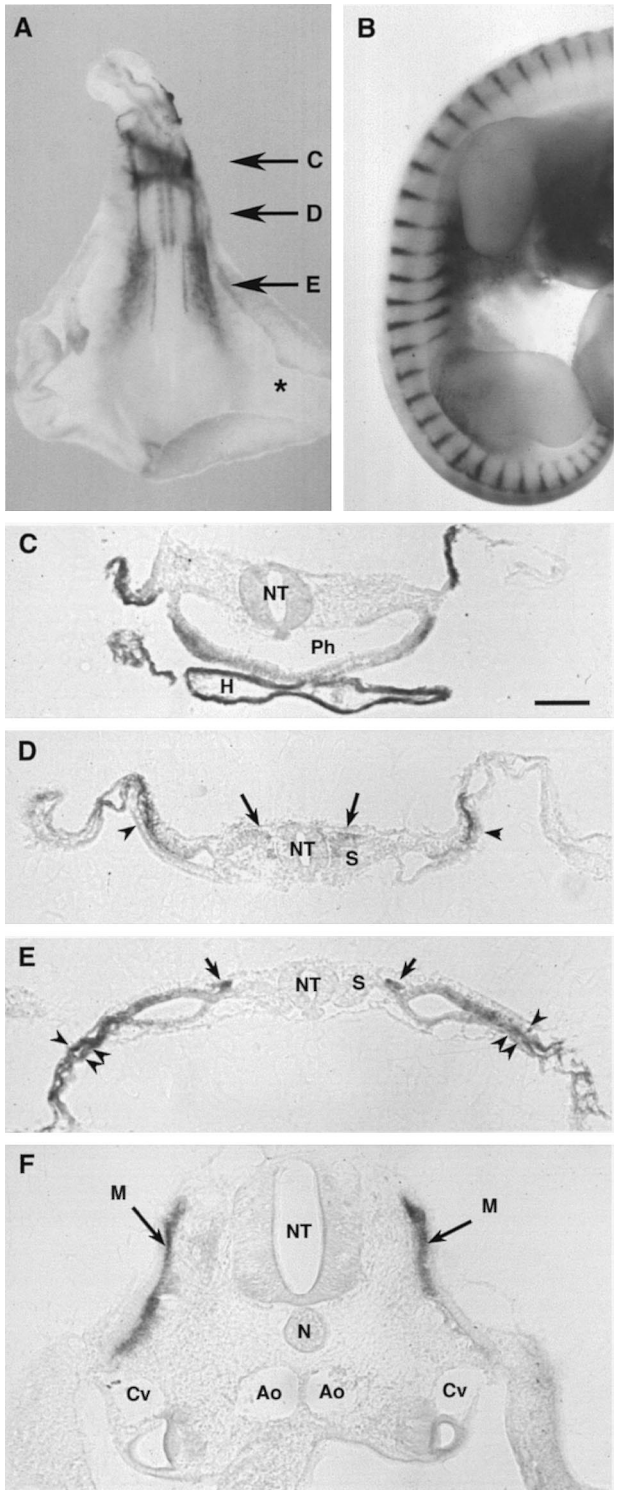

Figure 3 Onset of *qpim* expression. Wholemount *in situ* hybridization using *qpim* antisense riboprobe on E2 (**a**) and E3.5 (**b**) quail embryos. Levels of transverse sections shown in **c**, **d** and **e** are indicated in **a**. Note the absence of *qpim* expression in the yolk sac marked with an asterisk. In the E2 embryo, *qpim* is expressed (**c**) in the myocardium of the heart (H), (**d**) in the medial part of the somites (S; arrows), in the lateral mesoderm (arrowheads) and (**e**) in the Wolffian duct (arrows), somatopleura (arrowhead) and splanchnopleura (double arrowhead). (**f**) Transverse section through the trunk of the E3.5 embryo shown in **b**. Note *qpim* expression in the myotomes (M). NT: neural tube, N: notocord; Ph: pharynx; Ao: aorta; Cv: cardinal vein. Bar: 100 μm in **b**–**f**

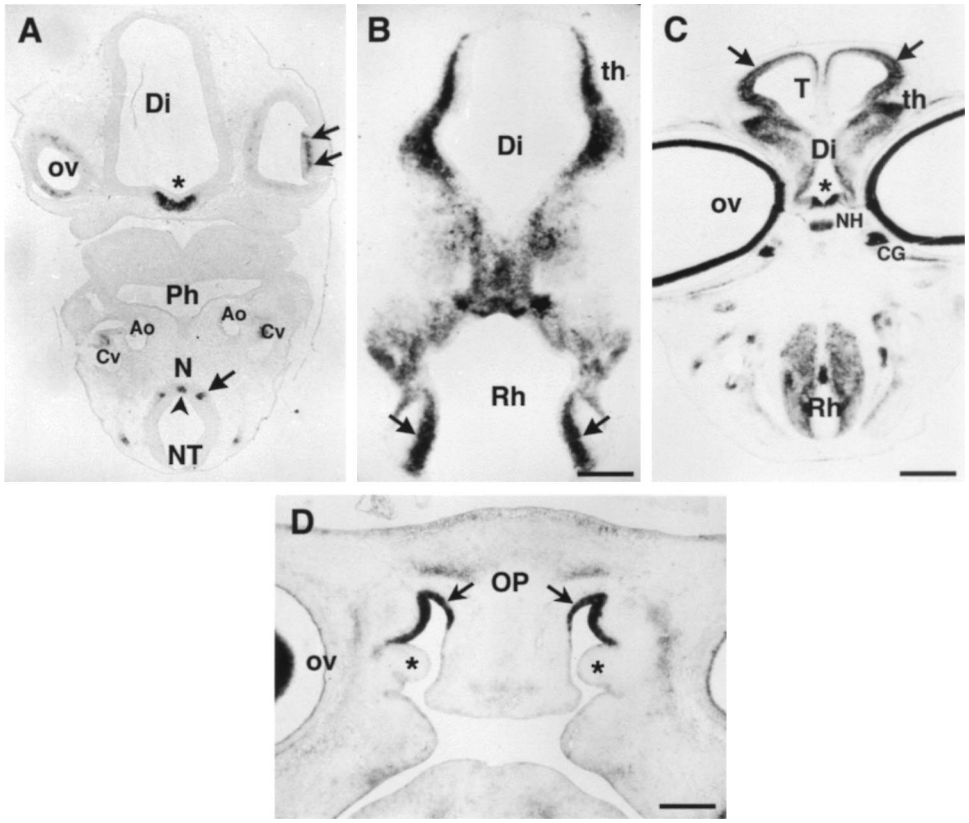

Figure 4 *qpim* expression in the developing nervous system. (**a**) Section through the diencephalon (Di) and optic vesicles (ov) of an E3.5 chick embryo. Note *qpim* expression in the hypothalamic infundibulum (asterisk) and in the developing lens (double arrow). At the level of the spinal cord, *qpim* is expressed in future motoneurons (arrow) and floor plate (arrowhead). (**b**–**d**) E5 quail embryo. (**b**) Section through the di- and rhombencephalon (Rh). Developing neuronal groups in the diencephalon correspond to the future Thalamus (th) and in the rhombencephalon to the nuclei of cranial nerve XII (arrows). (**c**) Section through the forebrain and rhombencephalon ventral to **b**. *qpim* is still expressed in the hypothalamic infundibulum (asterisk) and in the underlying neurohypophysis (NH). Neurons of the thalamus and of the cerebral cortex (arrows) express *qpim*. The developing neural retina and the PNS ciliary ganglion (CG) are strongly *qpim* positive. In the rhombencephalon, the floor plate is positive and a weaker signal is observed in differentiating neuroepithelial cells. (**d**) Section through the olfactory placode (OP) of an E5 quail embryo. *qpim* is strongly expressed in the olfactory epithelium (arrows), but not in the nasal epithelium (asterisks). Ao: aorta, Cv: cardinal vein; NT: neural tube, N: notochord, Ph: pharynx, T: telencephalon. Bars: **a**,**b** 280 μm, **c** 570 μm, **d** 330 μm

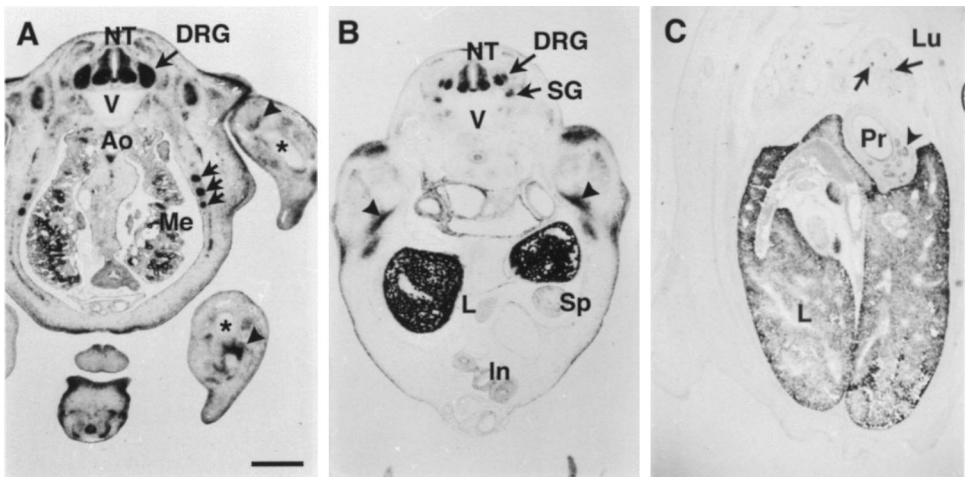

Figure 5 *qpim* expression in the abdominal region. (**a**, **b**) Transverse sections of E5 quail embryos. (**a**) Section at the level of the hindlimb. *qpim* is strongly expressed in the neural tube (NT), as well as in differentiating PNS neurons of the dorsal root ganglia (DRG) and sympathetic ganglia (SG). Expression is furthermore observed in tubules of the mesonephros (Me) and in cartilage condensations of the forming ribs (arrows), but not in the limbs (asterisks) or in the vertebrae (V). Myotomal cells of the limbs are still weakly *qpim* positive (arrowheads). (**b**) Section anterior to **a** at the level of the liver (L), which is highly *qpim* positive. By contrast, spleen (Sp) and intestine (In) do not express *qpim*. (**c**) Transverse section of an E7 chick embryo. Note strong expression in liver hepatocytes. *qpim* is also expressed in bronchi of the lung (Lu, arrows) and in secretory epithelium of the proventriculus (Pr, arrowhead). Bar: 600 μm in **a**–**c**

negative for *qpim* expression. In the peripheral nervous system (PNS), *qpim* expression was found in cranial as well as in dorsal root ganglia (DRG) and in sympathetic ganglia (Figures 4c and 5a,b).

qpim *transcripts in the abdominal region*

qpim was strongly expressed in kidney tubules until at least E10 (Figure 5a and data not shown). Furthermore, cartilage condensations of the forming ribs, but not the vertebrae or the limbs, were *qpim* positive (Figure 5a). Some weakly *qpim* positive cells could still be observed in the forming muscle masses of the limbs (Figure 5a,b). The strongest *qpim* signal in the developing embryo was observed in the liver hepatocytes of chicken and quail (Figure 5b,c). Expression in the liver persisted until E10 in the chicken and decreased afterwards (not shown). At E7, *qpim* expression was also detected in bronchi of the lung and in the secretory epithelium of the glandular stomach (Figure 5c). Quite unexpectedly, hematopoietic cells and tissues remained mostly *qpim* negative throughout the developmental period studied, with no expression e.g. in the yolk sac (Figure 3a), spleen (Figure 5b) or thymus (not shown). Only when we examined the spleen, thymus and bursa of Fabricius from E12 quail embryos, we could detect *qpim* expression in hematopoietic cells of the bursal follicles, but not in the other two organs (not shown).

pim-1, -2 *and* -3 *expression in the mouse embryo*

To be able to compare the expression pattern of *qpim* to those of the three known murine *pim* family genes, *pim-1*, *-2* and *-3* expression in mice was examined at three embryonic stages: E10, E14 and E17. At E10, neither *pim-2* nor *pim-3* were expressed at detectable levels (not shown), whereas *pim-1* was strongly expressed in the blood islands and in developing hematopoietic cells of the yolk sac (Figure 6a,b).

All three murine *pim* genes were expressed at E14 and E17, and are described here from the posterior to the cephalic end of the embryo. In the abdominal region, *pim-1* was strongly expressed in the liver at both E14 and E17 (Figure 6c). Histological examination showed that these cells likely belong to the hematopoietic compartment (not shown). At E17, scattered positive hematopoietic cells were also de-

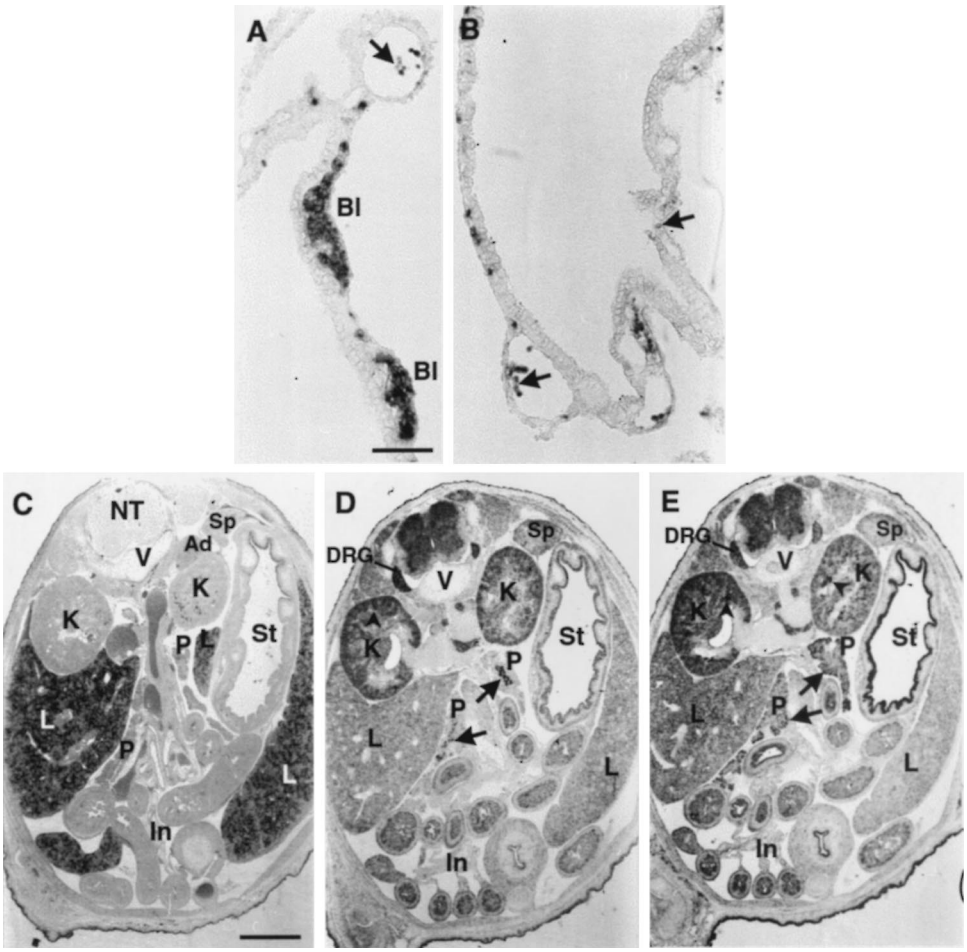

Figure 6 Expression of *pim-1*, *2* and *3* in mouse embryos. (**a**, **b**) Yolk sac of an E10 embryo probed with murine *pim-1*, which is expressed in the vast majority of hematopoietic cells of the blood islands (BI, **a**) and of the more mature vessels (**b**), although some negative cells can be observed (arrows). (**c**–**e**) Low magnification of transverse sections through the abdominal region of an E17 mouse embryo hybridized with *pim-1* (**c**), *-2* (**d**) and *-3* (**e**) antisense riboprobes. (**c**) *pim-1* expression is mainly detected in the liver (L). (**d**) *pim-2* expression is observed in the neural tube (NT), dorsal root ganglia (DRG), tubules of the cortical region of the kidney (K, arrowhead), the central duct of the pancreas (P, arrows) and some cells of the intestinal epithelium (In). (**e**) *pim-3* shares overlapping expression sites with *pim-1* in some cells of the liver, and with *pim-2* in neural tube, DRG, intestine, kidney (arrowheads) and pancreas (arrows). *Pim-3* alone is expressed in the epithelium of the stomach (St). Ad: adrenal gland; sp: spleen; V: vertebra. Bars: **a**,**b** 70 μm, **c**–**e** 600 μm

tected in the spleen (not shown). *pim-2* was not expressed in the liver or spleen, while some *pim-3* positive cells could be detected in the liver (Figure 6e), although they were much less abundant than *pim-1* positive cells. None of the three *pim* genes was expressed at detectable levels in the adrenal gland (Figure 6c and data not shown). *pim-2* expression was particularly strong in the epithelium of the main duct of the pancreas at both E14 (not shown) and E17 (Figure 6d) and appeared complementary to *pim-3*, which labeled cells at the periphery of this organ, corresponding to the precursors of acinar and islet cell epithelia (Figure 6e). Complementary expression patterns of *pim-2* and *-3* were also observed in the kidney: *pim-3* expression was strongest in the tubules of the medullary region, whereas *pim-2* was strongest in the cortical tubules (Figure 6d,e and data not shown). *pim-3* was the only of the three murine *pim* genes to be expressed in secretory epithelium of the stomach, and it also labeled the intestinal epithelium, some cells of which expressed *pim-2* (Figure 6d,e) and *pim-1* (not shown). All three *pim* genes were coexpressed in the surface ectoderm (Figures 6–9) of the E17 embryo.

The developing heart was negative for expression of the three murine *pim* genes at all three developmental stages examined (Figure 7 and data not shown). The lung showed no expression of *pim-1* (not shown), but overlapping expression of *pim-2* and *-3*: both genes were coexpressed in the main bronchi, while *pim-3* expression was in addition detected in all regions of the respiratory epithelium (Figure 7a,b). A significant site of *pim-1* expression in the E17 embryo was the thymus,

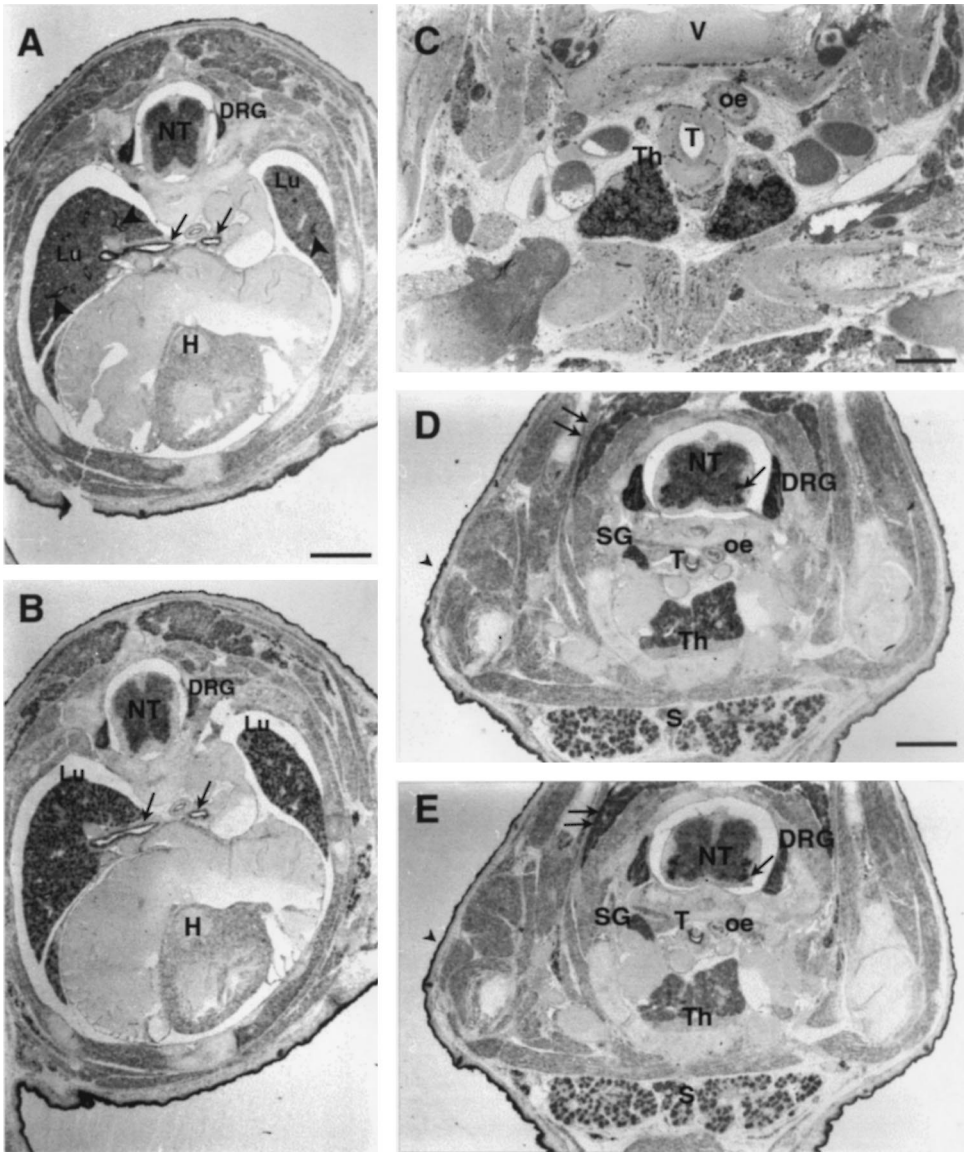

Figure 7 Expression of *pim-1*, *2* and *-3* in the thoracic region. (**a**, **b**) Transverse section through the lung (Lu) and heart (H) of an E17 embryo hybridized with *pim-2* (**a**) and *pim-3* (**b**) antisense riboprobes. Note expression of both genes in the neural tube and DRG. *pim-2* is expressed only in the main bronchi of the trachea (arrows) and the body of the lung (**a**), while *pim-3* is expressed in the remainder of the respiratory epithelium as well (**b**). (**c**–**e**) Transverse sections at the level of the thymus (Th) hybridized with *pim-1* (**c**), *pim-2* (**d**) and *pim-3* (**e**). All three genes are expressed in the thymus, albeit at different levels: *pim-1* labels numerous scattered cells in the medullary region (**c**), a weaker signal is detected throughout the thymus with *pim-2* (**d**), and *pim-3* is weakly expressed throughout the thymus (**e**). Note coexpression of *pim-2* and *-3* in DRG, sympathetic ganglia (SG) and motoneurons of the neural tube (arrow in **d** and **e**), as well as in the submandibular glands (S). All three genes are coexpressed in brown fat (double arrows) and in the surface ectoderm (arrowhead). V: vertebra, T: trachea, oe: oesophagus. Bars: **a,b,d,e** 600 μm, **c** 300 μm

where scattered *pim-1* positive cells were observed in the medullary region (Figure 7c). Both *pim-2* and *-3* were expressed in the thymus as well, albeit at different levels: weak expression of both genes was observed throughout the tissue (Figure 7d,e), with some strongly labeled *pim-2* positive cells (Figure 7d). Both *pim-2* and *-3* were also expressed in the submandibular glands (Figure 7d,e), where only few scattered *pim-1* positive cells were found (not shown).

Expression of pim-1, -2 *and* -3 *in the nervous system of mouse embryos*

Both *pim-2* and *3* showed a signal in the spinal cord neuroepithelium, DRG and sympathetic ganglia (Figures 6 and 7d,e). *pim-3* expression levels in the PNS were weaker than those of *pim-2*, and stronger in developing motoneurons. Murine *pim-1* expression was not observed in the spinal cord or PNS at any stage (e.g. Figure 6c). By contrast, murine *pim-1* was expressed in several discrete regions of the CNS at E17 (Figure 8). In the telencephalon, *pim-1* positive cells were detected in the cortical plate of the occipital lobe, corresponding to the region of the future visual cortex, as well as in the forming striatum (Figure 8a) and in the olfactory cortex (Figure 8c). Furthermore, the neural retina strongly expressed *pim-1* (Figure 8b), but showed only weak *pim-2* and *3* signals (not shown). *pim-2* and *-3* expression in the CNS was more widespread compared to *pim-1* and was observed in the ventricular zone of all brain regions (not shown).

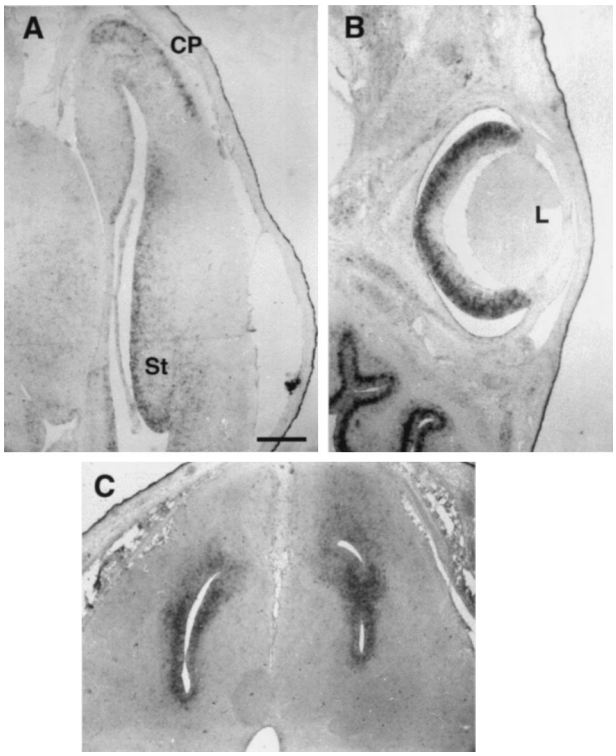

Figure 8 *pim-1* expression in the central nervous system of E17 mouse embryos. Dorsal side is up in all sections. (**a**) Transverse section at the level of the telencephalon with *pim-1* positive neurons localized in the striatum (St) and in the cortical plate (CP) of the occipital cortex. (**b**) Section through the eye, where neurons of the neural retina express *pim-1*. L: lens. (**c**) Section through the olfactory cortex. *pim-1* is expressed in the ventricular region. Bars: 300 μm in **a**–**c**

The most intriguing site of overlapping expression of the three murine *pim* kinase genes at the developmental stages examined in this study was the olfactory system. Neurons of the olfactory epithelium expressed both *pim-1* (Figure 9a,d) and *pim-3* (Figure 9b,e). The regions of the olfactory epithelium expressing these two kinases overlapped, although not completely (compare Figure 9a,b). The cellular layers expressing *pim-1* and *-3* also overlapped: neither kinase was expressed in the layer closest to the ventricle, which contains neuronal stem cells. *pim-1* was expressed in two cell layers containing differentiating and more mature neuroblasts (Figure 9d), while *pim-3* was only observed in the more mature neuroblast-containing layer (Figure 9b). Neither *pim-1* nor *-3* was expressed in the respiratory epithelium, which however expressed *pim-2* (Figure 9c,f). In the vomeronasal organ, both *pim-1* (Figure 9g) and *-3* (Figure 9h) were again coexpressed. *pim-2* showed a weaker signal in vomeronasal neurons, but was strongly expressed in the surrounding respiratory epithelium (Figure 9i).

Discussion

We here report cDNA cloning and functional characterization of the first member of the *pim* family of proto-oncogenes to be identified in birds. Alignment of the deduced amino acid sequence of the quail protein to the other members of the Pim kinase family revealed the highest degrees of homology to *Xenopus* Pim and to the recently identified rat Pim-3, whereas the mammalian Pim-1 and Pim-2 appeared evolutionary further diverged from these three. Qpim might thus represent the avian ortholog of Pim-3. However, since quail and *Xenopus* Pim proteins are not only highly homologous, but also completely colinear with each other, but not with rat Pim-3, it is still formally possible that Qpim represents yet a fourth member of the kinase family. Using *in vitro* kinase assays, we have been able to demonstrate that quail Qpim can phosphorylate itself as well as other proteins such as histone H1 and the NFATc1 transcription factor, which is one of the very few physiological substrates of Pim-1 identified so far (EM Rainio, J Sandholm and PJ Koskinen, in preparation). Our results thus indicate that we have identified from quail a functional Pim family serine/threonine kinase, which can share substrates with its murine relative Pim-1.

To date, very limited information has been available on the embryonic expression of *pim* genes. Therefore, we compared the expression patterns of *qpim* and mouse *pim-1*, *-2* and *-3* in developing avian and mouse embryos by *in situ* hybridization. Our analyses revealed that *qpim* expression in the developing avian embryo is not restricted to a particular cell type or organ, but includes derivatives from all three germ layers and is highly dynamic, especially at early developmental stages. No equivalent for the early stage expression pattern of *qpim* in mesodermal cells of the developing heart or the myotomes is observed in E10 mouse embryos probed with *pim-1*, *-2* or *-3*. The closest homolog of *qpim* in rodents, *pim-3*, is not expressed until E14, a stage which is comparable to E5 in the chick embryo. At these stages there are significant differences between the expression patterns of these

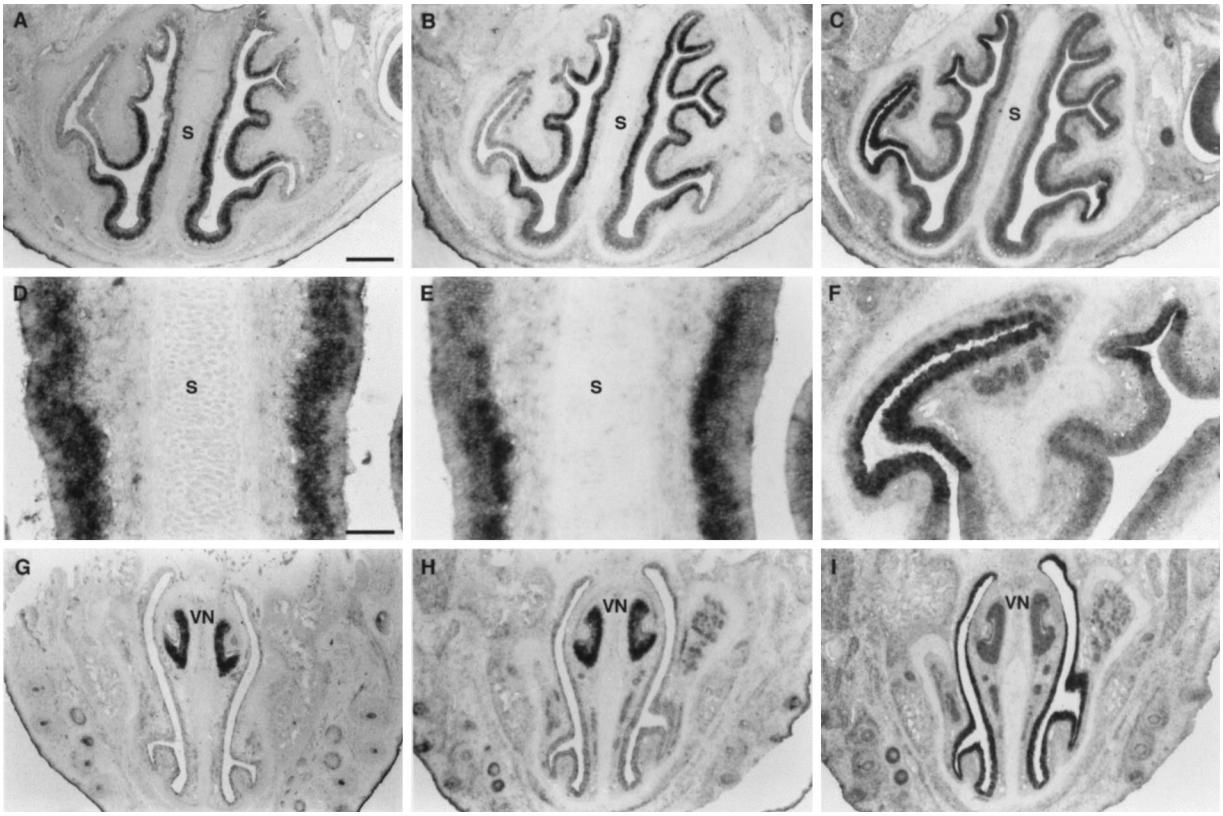

Figure 9 *pim-1*, *-2* and *-3* expression in the olfactory epithelium and vomeronasal organ. Transverse sections through the olfactory epithelium (**a**–**f**) and vomeronasal organ (**g**–**i**) hybridized with *pim-1* (**a**,**d**,**g**), *pim-3* (**b**,**e**,**h**) and *pim-2* (**c**,**f**,**i**). Dorsal side is up in all sections. The developing olfactory epithelium is strongly positive for *pim-1* (**a**) and *pim-3* (**b**), although the overlap is not complete. Notably, *pim-1* positive cells are localized in the intermediate layer of differentiating neurons, as well as in the layer of more mature neurons (**d**), while *pim-3* is expressed only in the latter (**e**). (**c**,**f**) *pim-2* is expressed only in respiratory epithelium, which is negative for *pim-1* and *-3*. (**g**–**i**) Sections through the vomeronasal organ (VN), which is strongly *pim-1* (**g**) and *pim-3* (**h**) positive at this stage. *pim-2* (**i**) is expressed at weaker levels in the VN, and labels strongly the respiratory epithelium. S: septum. Bars: **a**–**c**, **g**–**i** 300 μm, **d**–**f** 60 μm

two genes. Most notably, *qpim* is strongly expressed in the liver of an avian embryo, while much weaker signals are observed for *pim-3* in the same organ in a mouse embryo. Another site which shows significant differences is the CNS, where *qpim* strongly labels quite distinct neuronal populations, whereas murine *pim-3* is rather ubiquitously expressed, except in the olfactory epithelium, where intense signals for both genes are observed. This indicates that either the functions of the Pim-3 kinase have not been conserved during evolution, or that Qpim indeed represents a fourth member of the Pim family of kinases. To resolve this issue, we are in the process of cloning the mouse homolog of Qpim. It should be noted, however, that we have not detected mouse *pim-3* expression in the adrenal gland and heart, where it is strongly expressed in the adult (Feldman *et al*., 1998a,b). It is thus possible that the *pim-3* expression pattern evolves considerably during postnatal and adult life.

Our comparison of expression of the three murine *pim* genes during development has revealed several sites of potential Pim kinase function. During the developmental time window examined here, *pim-1* is unique among the murine *pim* genes to be expressed in all hematopoietic organs of the developing mouse embryo, including the yolk sac, liver, spleen and thymus. We have not yet characterized the precise cell types expressing *pim* genes, but histological examination of the liver indicates that the *pim-1* positive cells are hematopoietic cells. Interestingly, *pim-1* expression in the early erythrocytic cells of the yolk sac is in accordance with the decrease of erythrocyte mean cell volume observed in *pim-1*-deficient mice (Laird *et al*., 1993). Partially overlapping expression patterns are observed for the other two *pim* genes: *pim-3* is expressed in a subset of liver cells and both *pim-2* and *-3* in the thymus, but neither of them is detected in the spleen during the developmental time window examined. It should be noted that in adult mice *pim-2* has been reported to be coexpressed with *pim-1* in most hematopoietic tissues including thymus, spleen and bone marrow (Allen *et al*., 1997). Characterization of the cell types expressing the different *pim* genes might yield interesting information concerning the possible functional redundancy of Pim kinases in the hematopoietic compartment.

The expression patterns of *pim-2* and *-3* in the mouse embryo appear more closely related to each other than to *pim-1*. Interestingly, these two genes label different compartments of virtually all epithelia. These include the respiratory and digestive tract, excretory epithelium of the kidney and glandular epithelium of the pancreas. All three murine *pim* kinases are expressed in the surface ectoderm. The functional role of epithelial *pim* gene expression remains to be determined.

In the nervous system of mouse embryos, *pim-2* and *-3* are both strongly expressed in the PNS dorsal root and sympathetic ganglia. They are also coexpressed in

the spinal cord neuroepithelium, particularly in forming motoneuron columns. All of these structures appear *pim-1*-negative during the developmental time period examined. In contrast, in the forebrain, only *pim-1* is expressed in a localized manner, while *pim-2* and *-3* show rather ubiquitous, but weak expression. *pim-1* expression is detected at E17 in the telencephalon in the future olfactory and visual cortex. Interestingly, the neural retina and the olfactory epithelium including the vomeronasal organ are *pim-1* positive as well. While *pim-1* appears the only *pim* gene to be expressed in the visual system at these developmental stages, in the olfactory system, *pim-3* is expressed as well. Pim kinases might thus play a role in the perception of visual and olfactory stimuli, including the sensation of pheromones, which is localized in the vomeronasal organ (Herrada and Dulac, 1997). By contrast, *pim-2*, which has been reported to be strongly expressed in brain tissue of adult mice (Allen *et al*., 1997), was found only in the non-neuronal compartment of the olfactory system at the stages we examined. Further studies are clearly needed to compare the neuronal expression patterns of all three *pim* family genes, both during late stage embryogenesis and in adult tissues.

While our analyses were underway, intriguing findings on differential expression of *pim* family genes in adult rat hippocampus were reported. Both *pim-1* and *pim-3* are upregulated in specific regions of the hippocampus and cortex of rats upon synaptic activity, whereas *pim-2* is rather constitutively expressed there (Feldman *et al*., 1998a,b; Konietzko *et al*., 1999). Even more interestingly, induced expression of *pim-1* in the nuclear and dendritic compartments of hippocampal neurons is specifically required for long term potentiation, as shown by lack of such responses in *pim-1*-deficient mice (Konietzko *et al*., 1999). Taken together with our data, it has become evident that Pim kinases may have important, functionally redundant as well as non-redundant roles also outside of the hematopoietic system. Further studies including targeted inactivation of all three murine *pim* family genes are expected to shed more light on the role of the highly complex expression of various *pim* family genes and on the signal transduction pathways involving Pim kinases, especially in the central nervous system.

Materials and methods

Isolation and characterization of the qpim *cDNA*

We used an oligo-dT and random-primed amplified E4 quail embryo cDNA library (Invitrogen) available in our laboratory. Approximately 2×10^5 recombinant clones were screened on nitrocellulose filters (Schleicher & Schuell) with a radiolabeled PCR fragment of the human VEGF-B cDNA (sequence accession number U48801, Olofsson *et al*., 1996). Hybridization was performed at 42°C in a buffer containing 50% formamide, followed by washing at 42°C in $2 \times$ SSC/0.1%SDS. Among several positive clones isolated in the primary screen, one was purified and shown to contain an insert of 2.3 kb, which however failed to rehybridize with the VEGF-B probe. The *Eco*RI fragment containing this quail cDNA was transferred into the pcDNA3.1 vector (Invitrogen) and sequenced on both strands using the ABI Prism 310 genetic Analyzer (Perkin Elmer). Computer analyses of the sequences were carried out with the Fasta and Pileup programs of the Genetics Computer Group of the University of Wisconsin (Devereux *et al*., 1984).

In vitro *kinase assay*

The quail *qpim* cDNA was transferred into the pGEX-2T vector (Pharmacia) in frame with sequences encoding glutathione S-transferase. GST fusion proteins producing Qpim or mouse Pim-1 (EM Rainio, J Sandholm and PJ Koskinen, in preparation) were expressed in *E. coli*, attached to glutathione sepharose beads (Pharmacia) and incubated at 30°C for 30 min in 50 μl of kinase buffer (20 mM PIPES, pH 7.0, 5 mM $MnCl_2$, 7 mM β-mercaptoethanol, 0.4 mM spermine, 10 μM rATP) supplemented with 10 μCi [γ-^{32}P]ATP. Purified histone H1 (Sigma) or bacterially produced GST-NFATc1 fusion protein (aa 1-418; kindly provided by SN Ho) were added as exogenous substrates. Phosphorylated proteins were separated by SDS-polyacrylamide gel electrophoresis and visualized by autoradiography. The equivalent loading of GST fusion proteins was confirmed by Coomassie staining of the gel.

In situ *hybridization*

Sense and antisense riboprobes were prepared from the 2.3 kb *qpim* cDNA, from a 1.3 kb murine *pim-1* clone comprising the entire coding sequence as well as 330 bp and 100 bp of 5′ and 3′ UTR, respectively, from a 2.1 kb murine *pim-2* cDNA consisting of the coding sequence plus 0.9 kb of 3′UTR, and from a 1.2 kb murine *pim-3* partial cDNA spanning the 3′ half of the coding sequence together with 3′ UTR sequences. All the murine *pim* cDNAs were kindly provided by A Berns and H Mikkers. We used an *in vitro* transcription kit (Promega) and digoxygenin-labeled rUTP (Boehringer) according to the manufacturer's instructions. Murine *pim* probes were purified by spin-column chromatography on G-50 columns (Pharmacia). Wholemount *in situ* hybridizations were performed as described by Henrique *et al*. (1995). For sectioning of wholemounts, embryos were embedded in gelatin-sucrose, frozen and 20 μm cryostat sections were prepared as described in Pourquié *et al*. (1996). *In situ* hybridizations on paraffin sections (7.5 μm) of quail, chick or mouse embryos fixed in Serra's solution (60% EtOH, 30% formaldehyde, 10% acetic acid) were performed as described (Wilting *et al*., 1996). Briefly, sections were deparaffinated, rehydrated through a graded series of EtOH, rinsed in PBS and digested with proteinase K (Boehringer, 10 μg/ml) for 10 min at 37°C. After postfixation in 4% paraformaldehyde, sections were rinsed in $2 \times$ SSC and incubated overnight at 70°C in hybridization buffer (Henrique *et al*., 1995) containing 1 ng/μl riboprobe. Sections were washed in 50% formamide twice for 20 min at 65°C, and rinsed in MABT (100 mM maleic acid, 150 mM NaCl, pH 7.5, 0.1% Tween-20) twice for 20 min. Anti-Dig treatment and development of slides were performed as described in Henrique *et al*. (1995).

Acknowledgments

We thank Nicole Le Douarin and Luc Pardanaud for critical reading of the manuscript, Anton Berns, Harald Mikkers and Steffan Ho for reagents, Tapio Tainola and Hannakaisa Laakkonen for expert technical assistance, Gerard Couly and other members of the Institut d'Embryologie for helpful discussions and Francoise Viala and Francis Beaujean for the illustrations. This study was supported by grants from Association pour la Recherche contre le Cancer and Ligue Nationale contre le Cancer to the Institut d'Embryologie (A Eichmann) and the Academy of Finland (PJ Koskinen).

References

Acton D, Domen J, Jacobs H, Vlaar M, Korsmeyer S and Berns A. (1992). *Curr. Topics Microbiol. Immunol.,* **182,** 293–298.

Allen JD, Verhoeven E, Domen J, van der Valk M and Berns A. (1997). *Oncogene,* **15,** 1133–1141.

Amson R, Sigaux F, Przeborski S, Flandrin G, Givol D and Telerman A. (1989). *Proc. Natl. Acad. Sci. USA,* **86,** 8857–8861.

Breuer M, Slebos R, Verbeek S, van Lohuizen M, Wientjens E and Berns A. (1989). *Nature,* **340,** 61–63.

Cuypers HT, Selten G, Quint W, Zijlstra M, Robanus-Mandaag E, Boelens W, van Wezebeek P, Melief C and Berns A. (1984). *Cell,* **37,** 141–150.

Dautry F, Weil D, Yu J and Dautry-Varsat A. (1998). *J. Biol. Chem.,* **263,** 17615–17620.

Devereux J, Haeberli P and Smithies O. (1984). *Nucleic Acids Res.,* **12,** 387–395.

Domen J, van der Lugt NMT, Laird PW, Saris CJM, Clarke AR, Hooper ML and Berns A. (1993a). *Blood,* **82,** 1445–1452.

Domen J, van der Lugt NMT, Acton D, Laird PW, Linders K and Berns A. (1993b). *J. Exp. Med.,* **178,** 1665–1673.

Feldman JD, Vician L, Crispino M, Tocco G, Marcheselli VL, Bazan NG, Baudry M and Herschman HR. (1998a). *J. Biol. Chem.,* **273,** 16535–16543.

Feldman JD, Vician L, Crispino M, Tocco G, Baudry M and Herschman HR. (1998b). *J. Neurosci. Res.,* **53,** 502–509.

Henrique D, Adam J, Myat A, Chitnis A, Lewis J and Ish-Horowicz D. (1995). *Nature,* **375,** 787–790.

Herrada G and Dulac C. (1997). *Cell,* **90,** 763–773.

Hoover D, Friedmann M, Reeves R and Magnuson NS. (1991). *J. Biol. Chem.,* **266,** 14081–14083.

Konietzko U, Kauselmann G, Scafidi J, Staubli U, Mikkers H, Berns A, Schweizer M, Waltereit R and Kuhl D. (1999). *EMBO J.,* **18,** 3359–3369.

Laird PW, van der Lugt NMT, Clarke A, Domen J, McWhir J, Berns A and Hooper M. (1993). *Nucleic Acid Res.,* **21,** 4750–4755.

Leverson JD, Koskinen PJ, Orrico FC, Rainio EM, Jalkanen KJ, Dash AB, Eisenman RN and Ness SA. (1998). *Mol. Cell,* **2,** 417–425.

Lilly M, Le T, Holland P and Hendrickson SL. (1992). *Oncogene,* **7,** 727–732.

Lilly M and Kraft A. (1997). *Cancer Res.,* **57,** 5348–5355.

Lilly M, Sandholm J, Cooper JJ, Koskinen PJ and Kraft A. (1999). *Oncogene,* **18,** 4022–4031.

Matikainen S, Sareneva T, Ronni T, Lehtonen A, Koskinen PJ and Julkunen I. (1999). *Blood,* **93,** 1980–1991.

Meeker TC, Nagarajan L, ar-Rushdi A, Rovera G, Huebner K and Croce CM. (1987). *Oncogene Res.,* **1,** 87–101.

Möröy T, Verbeek S, Ma A, Achaoso P, Berns A and Alt F. (1991). *Oncogene,* **6,** 1941–1948.

Möröy T, Grzeschiczek A, Petzold S and Hartmann KU. (1993). *Proc. Natl. Acad. Sci. USA,* **90,** 10734–10738.

Olofsson B, Pajusola K, Kaipainen A, von Euler G, Joukov V, Saksela O, Orpana A, Petterson RF, Alitalo K and Eriksson V. (1996). *Proc. Natl. Acad. Sci. USA,* **93,** 2576–2581.

Pourquié O, Fan CM, Coltey M, Hirsinger E, Watanabe Y, Bréant C, Francis-West P, Brickell P, Tessier-Lavigne M and Le Douarin NM. (1996). *Cell,* **84,** 461–471.

Saris CJM, Domen J and Berns A. (1991). *EMBO J.,* **10,** 655–664.

Selten G, Cuypers HT and Berns A. (1985). *EMBO J.,* **4,** 1793–1798.

Sorrentino V, McKinney MD, Giori M, Geremia R and Fleissner E. (1988). *Proc. Natl. Acad. Sci. USA,* **85,** 2191–2195.

te Riele H, Robanus-Maandag E, Clarke A, Hooper M and Berns A. (1990). *Nature,* **348,** 649–651.

van der Lugt NMT, Domen J, Verhoeven E, Linders K, van der Gulden H, Allen J and Berns A. (1995). *EMBO J.,* **14,** 2536–2544.

van Lohuizen M, Verbeek S, Krimpenfort P, Domen J, Saris C, Radaskiewicz T and Berns A. (1989). *Cell,* **56,** 673–682.

Verbeek S, van Lohuizen M, van der Valk M, Domen J, Kraal G and Berns A. (1991). *Mol. Cell. Biol.,* **11,** 1176–1179.

Wilting J, Birkenhäger R, Eichmann A, Kurz H, Martiny-Baron G, Marmé D, McCarthy J, Christ B and Weich H. (1996). *Dev. Biol.,* **176,** 76–85.

Wingett D, Reeves R and Magnuson NS. (1992). *Nucleic Acid Res.,* **20,** 3183–3189.

Wingett D, Long A, Kelleher D and Magnuson NS. (1996). *J. Immunol.,* **156,** 549–557.